Galactic Parameters from Masers with Trigonometric Parallaxes

Vadim V. Bobylev and Anisa T. Bajkova

Central Astronomical Observatory at Pulkovo of RAS, Pulkovskoye Chaussee 65/1, 196140, Saint-Petersburg, Russia.
E-mail: vbobylev@gao.spb.ru, anisabajkova@rambler.ru

ABSTRACT

Spatial velocities of all currently known 28 masers having trigonometric parallaxes, proper motion and line-of-site velocities are reanalyzed using Bottlinger's equations. These masers are associated with 25 active star-forming regions and are located in the range of galactocentric distances $3 < R < 14$ kpc. To determine the Galactic rotation parameters, we used the first three Taylor expansion terms of angular rotation velocity Ω at the galactocentric distance of the Sun $R_0 = 8$ kpc. We obtained the following solutions: $\Omega_0 = -31.0 \pm 1.2$ km s^{-1}kpc^{-1}, $\Omega_0' = 4.46 \pm 0.21$ km s^{-1} kpc^{-2}, $\Omega_0'' = -0.876 \pm 0.067$ km s^{-1} kpc^{-3}, Oort constants: $A = 17.8 \pm 0.8$ km s^{-1} kpc^{-1}, $B = -13.2 \pm 1.5$ km s^{-1} kpc^{-1} and circular velocity of the Solar neighborhood rotation $V_0 = 248 \pm 14$ km s^{-1}. Fourier analysis of galactocentric radial velocities of masers V_R allowed us to estimate the wavelength $\lambda = 2.0 \pm 0.2$ kpc and peak velocity $f_R = 6.5 \pm 2$ km s^{-1} of periodic perturbations from the density wave and velocity of the perturbations 4 ± 1 km s^{-1} near the location of the Sun. Phase of the Sun in the density wave is estimated as $\chi_\odot \approx -130^o \pm 10^o$. Taking into account perturbations evoked by spiral density wave we obtained the following non-perturbed components of the peculiar Solar velocity with respect to the local standard of rest (LSR) $(U_\odot, V_\odot, W_\odot)_{\rm LSR} = (5.5, 11, 8.5) \pm (2.2, 1.7, 1.2)$ km s^{-1}.

Key words: Masers – SFRs – Spiral Arms: Rotation Curve – Galaxy (Milky Way).

1 INTRODUCTION

Study of Galactic parameters, especially of the Galactic rotation curve, is of great importance in solving a number of problems, such as estimating the mass of the Galaxy, determining the distribution of matter, estimating the hidden mass, studying dynamics and structure of the Galaxy and its subsystems, etc.

For this purpose masers having trigonometric parallaxes, line-of-sight velocities and proper motions (Reid et al., 2009) are of great interest. Currently measurements of parallaxes with mean error of several percents are fulfilled with radio interferometers for three tens of masers in the various active high-mass star-forming regions. Because these masers are associated with very young ($< 10^5$ yr) OB stars, their kinematics reflects the properties of the youngest part of the Galactic disk.

Analysis of motions of 18 masers was made by a number of authors (Reid et al., 2009; Baba et al., 2009; Bovy et al., 2009; McMillan & Binney, 2010). For the first time Reid et al. (2009) suggested that high-mass star-forming regions significantly (≈ 15 km s^{-1}) lag circular rotation. McMillan

& Binney (2010) suggest that much of this lag could be accounted for by increasing the value of the Solar motion in the direction of galactic rotation from 5 to 11 km s^{-1}.

The question of particular interest is the peculiar velocity of the Sun with respect to the LSR, $(U_\odot, V_\odot, W_\odot)_{\rm LSR}$. On the basis of Strömberg's relation, Dehnen & Binney (1998) determined the vector $(U_\odot, V_\odot, W_\odot)_{\rm LSR} = (10.0, 5.3, 7.2) \pm (0.4, 0.6, 0.4)$ km s^{-1} using proper motions of $\approx$12000 main sequence stars from the Hipparcos catalogue. These results were confirmed by Aumer & Binney (2009): $(U_\odot, V_\odot, W_\odot)_{\rm LSR} = (10.0, 5.3, 7.1) \pm (0.3, 0.5, 0.3)$ km s^{-1}, who applied the same method to proper motions from the revised version of the Hipparcos catalogue (van Leeuwen, 2007). In the work of Schönrich et al. (2010), where gradient of metallicity of stars in the Galactic disk was taken into account, this velocity is different: $(U_\odot, V_\odot, W_\odot)_{\rm LSR} = (11.1, 12.2, 7.3) \pm (0.7, 0.5, 0.4)$ km s^{-1}. Using another approach, Francis & Anderson (2009) suggested that this velocity is: $(U_\odot, V_\odot, W_\odot)_{\rm LSR} = (7.5, 13.5.2, 6.8) \pm (1.0, 0.3, 0.1)$ km s^{-1}.

In the present work, we are trying to establish relationship between motions of all currently known masers having

parallaxes, proper motions and line-of-sight velocities, and parameters of the Galactic spiral density waves (Lin & Shu, 1964), and to estimate components of the peculiar velocity of the Sun with respect to the LSR. This goal is achieved by determining parameters of the Galactic rotation curve, as well as other kinematic parameters, by means of Bottlinger's equations. Fourier analysis of periodic deviations of observational velocities of masers from the Galactic rotation curve is aimed to obtain some estimates of spiral density wave parameters.

2   DATA

Input data on methanol masers with trigonometric parallaxes and proper motions from VLBI measurements are taken from the papers of Reid et al. (2009), Rygl et al. (2010). We added also H_2O masers SVS 13 in NGC 1333 (Hirota et al., 2008a), IRAS 22196+6336 in Lynds 1204G (Hirota et al., 2008b) and G14.33–0.64 (Sato et al., 2010), with parallaxes and proper motions measured in the framework of VERA (VLBI Exploration of Radio Astrometry) program. Note that, for maser NGC 281–W listed in Reid et al. (2009), we used observational data obtained by Rygl et al. (2010) with the quoted uncertainty for 6.7 GHz masers smaller than the Sato et al. (2008) 22 GHz masers. For the nearest star-forming region in Orion, along with the data on maser Orion–KL (Hirota et al., 2007), we use independent VLBA observations of radio star GMR A (Sandstrom et al., 2007) with line-of-sight velocity with respect to the LSR $(V_r)_{LSR} = -4 \pm 5$ km s^{-1} (Bower et al., 2003). It is the Bower's et al. (2003) opinion that the GMR A source is a young star of T Tau type (WTTS). We use also a very young object a supergiant S Per (Asaki et al., 2007) with line-of-sight velocity $V_r = -39.7 \pm 0.7$ km s^{-1} from Famaey et al. (2005).

All 28 objects being studied are listed in Table 1. In Fig. 1, one can see only 25 points because X, Y coordinates of some objects are very close to each other. For example, three masers Cep A, IRAS 22198 and L 1206 form practically a single point in the XY plane.

Fig. 1 is drawn in galactocentric Cartesian coordinates X and Y. As one can see from this picture, only one maser has inaccurately measured parallax. That is the maser W51 (in the first Galactic quadrant), with relative error of parallax $e_\pi/\pi = 0.36$. In fact, only this maser requires calculation of upper and lower bounds on its distance. But, because this maser lies in the horizontal part of the Galactic rotation curve, hereafter we use an average estimate of the heliocentric distance $r \pm \sigma_r$ or galactocentric distance $R \pm \sigma_R$. The same distance estimates are used also for other masers.

We reduce line-of-sight velocities of masers with respect to the LSR to the heliocentric coordinate system using the standard Solar motion velocity: $(\alpha, \delta)_{1900} = (270°, +30°)$, $V = 20$ km s^{-1}, hence $(U_\odot, V_\odot, W_\odot)_{LSR} = (10.3, 15.3, 7.7)$ km s^{-1} (Reid et al., 2009).

It is very important for the purposes of our study to know the accurate value of R_0. A review of R_0 estimates made by a number of authors can be found in the paper by Avedisova (2005), where the average value is derived as $R_0 = 7.80 \pm 0.33$ kpc. Note that the most reliable values of this parameter were obtained only recently. Analysis of
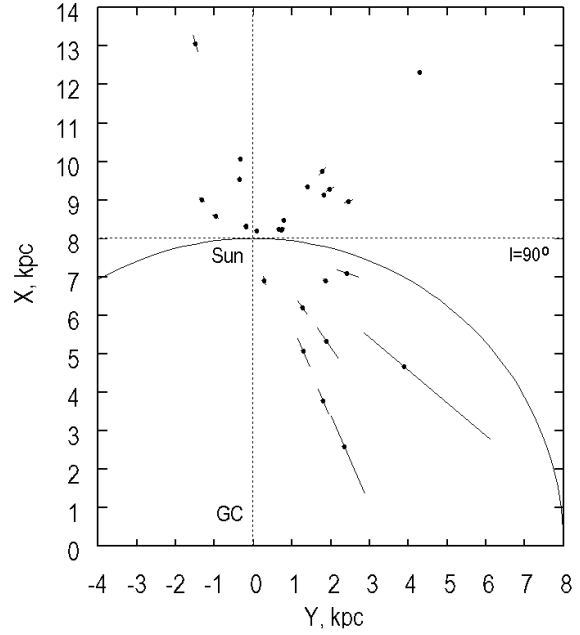
Figure 1. Coordinates of masers in the XY Galactic plane. Locations of the Sun and Galactic Centre (GC) are indicated. The circle of 8 kpc radius is drawn.

motion of the star S2 around the black hole in the Galactic Centre gave $R_0 = 8.4 \pm 0.4$ kpc (Ghez et al., 2008). This value is in a good agreement with observations of orbits of 28 stars near the Galactic Centre during 16 yr: $R_0 = 8.31 \pm 0.33$ kpc (Gillessen et al., 2009).

In general, modern estimations show that the most probable value of R_0 is close to 8.0 kpc, and error of its determination is close to 0.3 kpc. For the sake of reliability, we'll consider that the value of R_0 lies in the $7.5 - 8.5$ kpc range.

3   METHODS

3.1   Determining Rotation Curve Parameters

Method used here is based on the well-known Bottlinger's formulas (Ogorodnikov, 1958), where angular velocity of Galactic rotation is expanded in a series to n-th order terms in r/R_0:

$$V_r = -u_\odot \cos b \cos l - v_\odot \cos b \sin l - w_\odot \sin b - \quad (1)$$
$$-R_0 \sin l \cos b[(R - R_0)\Omega_0^1/1! + \ldots + (R - R_0)^n \Omega_0^n/n!],$$

$$V_l = u_\odot \sin l - v_\odot \cos l + r\Omega_0 \cos b - \quad (2)$$
$$-(R_0 \cos l - r \cos b)[(R - R_0)\Omega_0^1/1! +$$
$$+ \ldots + (R - R_0)^n \Omega_0^n/n!],$$

$$V_b = u_\odot \cos l \sin b + v_\odot \sin l \sin b - w_\odot \cos b + \quad (3)$$
$$+R_0 \sin l \sin b[(R - R_0)\Omega_0^1/1! + \ldots + (R - R_0)^n \Omega_0^n/n!],$$

where V_r is heliocentric line-of-sight velocity; $V_l = 4.74r\mu_l \cos b$ and $V_b = 4.74r\mu_b$ are proper motion velocity components in the l and b directions, respectively (the coefficient 4.74 is the quotient of the number of kilometers in astronomical unit by the number of seconds in a tropical year); $r = 1/\pi$ is the heliocentric distance of an object;

Table 1. Data on masers. Velocities U^1, V^1, W^1 are residual velocities with Galactic rotation excluded using parameters (16).

Source	R, kpc	U^1, km s^{-1}	V^1, km s^{-1}	W^1, km s^{-1}	ΔV_θ, km s^{-1}	V_R, km s^{-1}	Ref
L 1287	8.52	-2.9 ± 1.7	-20.7 ± 2.6	-10.2 ± 2.5	-5.7 ± 2.6	-5.6 ± 1.7	(2)
IRAS 00420+5530	9.33	3.0 ± 2.7	-19.6 ± 4.2	-1.5 ± 0.8	-2.9 ± 4.2	-11.8 ± 2.8	(1)
NGC 281–W	9.50	-4.2 ± 2.6	-2.3 ± 2.8	-16.0 ± 1.7	12.8 ± 2.8	-1.2 ± 2.6	(2)
W3 (OH)	9.46	4.8 ± 2.1	-17.6 ± 2.2	-6.2 ± 0.2	-1.2 ± 2.2	-13.1 ± 2.1	(1)
WB 89–437	13.05	0.2 ± 2.1	-17.1 ± 2.1	2.5 ± 3.8	0.2 ± 2.1	-8.6 ± 2.1	(1)
NGC 1333 (f1)	8.21	-23.6 ± 4.4	-13.5 ± 2.3	0.0 ± 2.5	0.9 ± 2.3	15.6 ± 4.4	(3)
NGC 1333 (f2)	8.21	-21.1 ± 4.5	5.5 ± 1.8	10.0 ± 3.5	20.0 ± 1.8	13.3 ± 4.5	(3)
Ori GMR A	8.32	-4.7 ± 4.1	-8.8 ± 2.3	-3.1 ± 1.7	5.6 ± 2.3	-3.4 ± 4.1	(4)
Ori KL	8.34	-17.9 ± 4.2	-14.4 ± 2.4	-3.8 ± 3.0	0.3 ± 2.4	9.9 ± 4.2	(1)
S252 A	10.08	-12.6 ± 3.0	-11.1 ± 0.6	-9.2 ± 0.3	3.5 ± 0.6	4.5 ± 3.0	(1)
S255	9.56	-7.7 ± 3.6	-0.8 ± 9.5	-4.0 ± 10	13.7 ± 9.5	-0.8 ± 3.6	(2)
S269	13.16	-3.5 ± 2.9	-16.2 ± 1.2	-11.7 ± 0.9	-2.2 ± 1.2	-4.3 ± 2.9	(1)
VY CMa	8.64	-6.1 ± 2.9	-16.9 ± 3.0	-13.6 ± 2.5	-2.7 ± 3.0	-1.6 ± 2.9	(1)
G232.62+0.9	9.12	-7.8 ± 3.2	-10.5 ± 3.1	-6.4 ± 2.2	4.0 ± 3.1	-0.9 ± 3.2	(1)
G14.33−0.64	6.92	0 ± 10	-10 ± 14	-10.8 ± 4.5	5 ± 14	-8 ± 10	(1)
G23.66−0.13	5.23	21.6 ± 3.7	-6.7 ± 5.7	-3.1 ± 0.4	14.8 ± 5.6	-26.8 ± 3.8	(1)
G23.01−0.41	4.18	1.0 ± 4.7	-20.7 ± 9.1	-8.5 ± 2.3	-1.8 ± 8.4	-10.8 ± 5.8	(1)
G23.43−0.18	3.50	-15 ± 10	9 ± 22	-5.3 ± 1.8	13 ± 18	20 ± 16	(1)
G35.20−0.74	6.34	-21.7 ± 3.3	-20.1 ± 3.6	-15.7 ± 1.5	-8.2 ± 3.6	12.2 ± 3.3	(1)
W48	5.65	-31.1 ± 5.7	-16.5 ± 7.5	-16.5 ± 2.4	-9.6 ± 7.3	21.1 ± 5.9	(1)
W51	6.08	-24 ± 41	-10 ± 35	-10.4 ± 3.7	-7 ± 37	15 ± 38	(1)
V645	7.16	-14.4 ± 2.6	-13.6 ± 2.9	-11.4 ± 0.5	-0.8 ± 2.9	6.3 ± 2.6	(1)
Onsala1	7.50	-9 ± 13	-18.3 ± 5.6	-2.9 ± 6.0	-4.1 ± 6.8	0 ± 12	(2)
IRAS 22198	8.26	-4.2 ± 3.7	-23.4 ± 4.9	3.0 ± 2.1	-8.6 ± 4.9	-4.6 ± 3.7	(3)
L 1206	8.27	-12.8 ± 4.4	-19.4 ± 3.2	-7.2 ± 5.7	-5.3 ± 3.2	4.4 ± 4.3	(2)
Cep A	8.26	-8.9 ± 3.8	-16.6 ± 4.9	-12.6 ± 1.2	-2.2 ± 4.8	0.7 ± 3.8	(1)
NGC 7538	9.30	-2.1 ± 2.1	-32.7 ± 2.9	-18.1 ± 1.0	-16.0 ± 2.8	-10.5 ± 2.2	(1)
S Per	9.30	-16.1 ± 1.2	-16.9 ± 1.2	-17.2 ± 3.1	-3.9 ± 1.1	7.5 ± 1.1	(5)

Notes. Initial data are taken from: (1) – Reid et al. (2009); (2) – Rygl et al. (2010); (3) – Hirota et al. (2008a); (4) – Sandstrom et al. (2007); (5) – Asaki et al. (2007).

proper motion components $\mu_l \cos b$ and μ_b are in mas yr^{-1}, line-of-sight velocity V_r is in km s^{-1}; $u_\odot, v_\odot, w_\odot$ are Solar velocity components with respect to the mean group velocity under consideration; R_0 is the galactocentric distance of the Sun; R is the galactocentric distance of an object; R, R_0 and r are in kpc. Velocity U directed towards the Galactic Centre, V along the Galactic rotation, and W towards the Northern Galactic pole. The quantity Ω_0 is the Galactic angular rotational velocity at distance R_0, parameters $\Omega_0^1, \ldots, \Omega_0^n$ are derivatives of the angular velocity from the first to the n-th order, respectively. The distance R can be calculated using the expression

$$R^2 = r^2 \cos^2 b - 2R_0 r \cos b \cos l + R_0^2. \quad (4)$$

The system of conditional equations (1)–(3) contains $n + 4$ unknowns: $u_\odot, v_\odot, w_\odot, \Omega_0, \Omega_0^1, \ldots, \Omega_0^n$, which can be determined by the least-squares method. The system of equations (1)–(3) is solved with weights of the form

$$P_{(r,l,b)} = S_0 / \sqrt{S_0^2 + \sigma_{V_{r,l,b}}^2}, \quad (5)$$

where P_r, P_l and P_b are the weights of equation for V_r, V_l and V_b correspondingly, and $S_0 = 8$ km s^{-1} is the "cosmic" dispersion averaged over all observations. Errors σ_{V_l} and σ_{V_b} of velocities V_l and V_b can be calculated using the formulas

$$\sigma_{(V_l, V_b)} = 4.74 r \sqrt{\mu_{l,b}^2 \left(\frac{\sigma_\pi}{\pi} \right)^2 + \sigma_{\mu_{l,b}}^2}. \quad (6)$$

3.2 Determining Projections V_θ and V_R

Components of spatial velocities U, V, W of masers are determined from observed radial (line-of-sight) and tangential velocities V_r, V_l, V_b in the following way:

$$U = V_r \cos l \cos b - V_l \sin l - V_b \cos l \sin b,$$
$$V = V_r \sin l \cos b + V_l \cos l - V_b \sin l \sin b, \quad (7)$$
$$W = V_r \sin b + V_b \cos b.$$

Then we find two projections of these velocities: V_R, directed radially from the Galactic Centre towards an object, and V_θ, orthogonal to V_R and directed towards Galactic rotation:

$$V_\theta = U \sin \theta + (V_0 + V) \cos \theta, \quad (8)$$
$$V_R = -U \cos \theta + (V_0 + V) \sin \theta, \quad (9)$$

where $V_0 = |R_0 \Omega_0|$, and position angle θ is determined as $\tan \theta = y/(R_0 - x)$, where x, y are Galactic Cartesian coordinates of an object. In addition, it is assumed that velocities U and V are free from the Solar velocity with respect to mean group velocity $(u_\odot, v_\odot, w_\odot)$ obtained from equations (1)–(3). Errors of projections V_R and V_θ are estimated from the expressions

$$\sigma^2(V_\theta) = \sigma_U^2 \sin^2 \theta + \sigma_V^2 \cos^2 \theta, \quad (10)$$
$$\sigma^2(V_R) = \sigma_U^2 \cos^2 \theta + \sigma_V^2 \sin^2 \theta, \quad (11)$$

where errors of spatial velocities U and V are denoted by σ_U and σ_V, respectively.

We are interested also in heliocentric spatial velocities
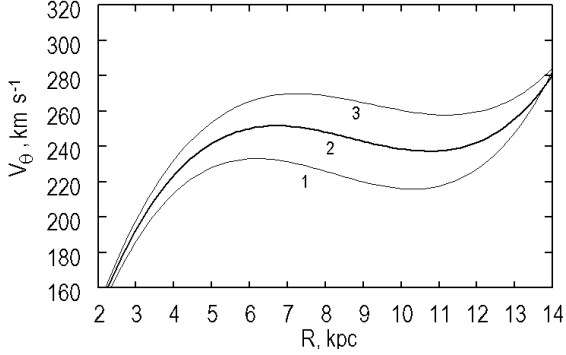
Figure 2. Galactic rotation curves $V_\theta(R)$ for adopted $R_0 = 7.5, 8.0, 8.5$ kpc, lines 1,2 and 3.

which are free from Galactic rotation with parameters (16) but not from Solar velocity. We denote such velocities by U^1, V^1, W^1 (see Table 1 and Fig. 7). These velocities must satisfy the following equations:

$$\overline{U}^1 = -u_\odot, \quad \overline{V}^1 = -v_\odot, \quad \overline{W}^1 = -w_\odot. \qquad (12)$$

3.3   Fourier Analysis of Velocities

At the next step, we consider deviations from circular velocities ΔV_θ and galactocentric radial velocities V_R.

Spectral analysis consists in applying direct Fourier transform to the sequence of residual velocities following way:

$$\overline{V}(\lambda_k) = \frac{1}{M} \sum_i^M V^i \exp\left(-j\frac{2\pi}{\lambda_k} R_i\right), \qquad (13)$$

where $\overline{V}(\lambda_k)$ is the k-th harmonic of Fourier transform, M is the number of measurements of velocities V^i with coordinates R_i, $i = 1, 2, \ldots, M$, and λ_k is wavelength in kpc; the latter is equal to D/k, where D is the period of the original sequence in kpc. In density wave theory, λ denotes the distance between adjacent spiral arms along the Galactic radius vector.

Understanding the results of spectral analysis is easy in the framework of linear theory of density waves. According to this approach (Burton & Bania, 1974; Byl & Ovenden, 1978),

$$V_R = -f_R \cos\chi, \qquad (14)$$
$$\Delta V_\theta = f_\theta \sin\chi, \qquad (15)$$

where $\chi = m[\cot(i)\ln(R/R_0) - \theta] + \chi_\odot$ is phase of the spiral wave (m is number of spiral arms, i is pitch angle, $\chi_\odot$ is the phase of the Sun in the spiral wave (Rohlfs, 1977)); f_R and f_θ are amplitudes of radial and tangential components of the perturbed velocities which, for convenience, are always considered positive.

For the case when perturbations V_R and ΔV_θ are considered as periodic functions of logarithm of R, the following expression for the phase is appropriate: $\chi = (2\pi R_0/\lambda)\ln(R/R_0) + \chi_\odot \approx (2\pi/\lambda)(R - R_0) + \chi_\odot$ (Mel'nik et al, 2001), what allows us to use Fourier analysis (13).

In our coordinate system radial velocity V_R is directed
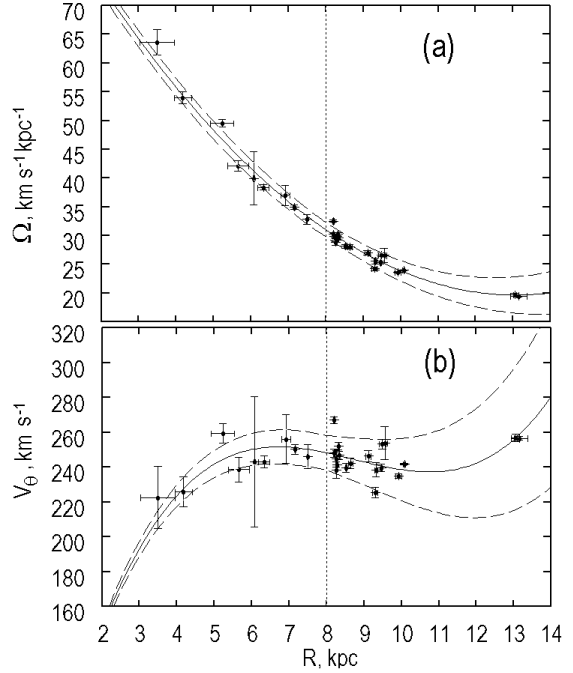
Figure 3. (a) Rotational angular velocity and (b) rotational circular linear velocity of the Galaxy according to (16) versus galactocentric distance. Dashed lines denote the bounds of the confidence interval corresponding to the 1σ level. Vertical line indicates the location of $R_0 = 8$ kpc.

from galactic centre and circular velocity deviation ΔV_θ directed along Galactic rotation. Centre of the spiral arm corresponds to phase $\chi = 0$. For definiteness (Rohlfs, 1977), we consider that the centre of the Carina–Sagittarius arm ($R \approx 7$ kpc) corresponds to phase $\chi = 0$, while the Perseus arm ($R \approx 9$ kpc) corresponds to phase $\chi \approx -\frac{3}{2}\pi$.

4   RESULTS

4.1   Galactic Rotation Curve

Firstly we investigated solutions of equations (1)–(3) using the different number of Taylor expansion terms of Ω for different values of R_0. Direct construction of the rotation curve using the rotation parameters obtained above showed that every additional expansion term leads to significant widening of the confidence interval. We revealed that it is enough to take three terms of Taylor expansion to construct a smooth, sufficiently accurate Galactic rotation curve in the galactocentric distance range of $3 < R < 14$ kpc. Indeed, adding subsequent terms to the expansion practically does not change the shape of the curve, and additional terms do not differ statistically from zero. So, in this sense we found the optimal solution. Results of this study are shown in Fig. 2, whence we can see that the shape of the rotation curve significantly depends on the adopted value of R_0. Thus, variation $dR_0 = 0.5$ kpc leads to variation of the rotational angular velocity $dV_\theta \approx 20$ km s^{-1}. As one can see from Fig. 2, influence of inaccuracy in R_0 is particularly strong in the Solar neighborhood.

Then we obtained solution of (1)–(3) for the fixed value of $R_0 = 8.0$ kpc for 84 equations. As a result we
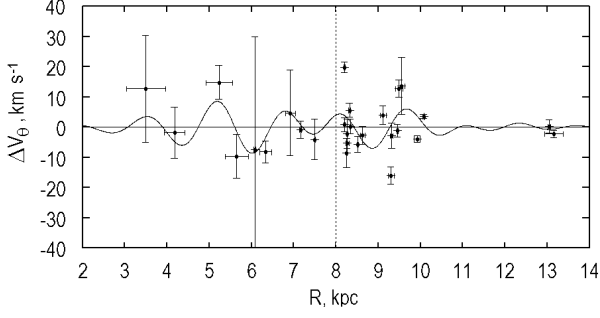
Figure 4. Deviations from circular velocities ΔV_θ after subtraction of the model rotation curve with parameters (16) versus galactocentric distance; vertical line indicates $R_0 = 8$ kpc.

found the following parameters of the Solar velocity with respect to the group velocity: $(u_\odot, v_\odot, w_\odot) = (8.0, 14.9, 7.6) \pm (2.1, 1.9, 1.6)$ km s^{-1}, and parameters of the angular velocity of Galactic rotation:

$$\Omega_0 = -31.0 \pm 1.2 \text{ km s}^{-1}\text{kpc}^{-1}, \quad (16)$$
$$\Omega_0' = +4.46 \pm 0.21 \text{ km s}^{-1}\text{kpc}^{-2},$$
$$\Omega_0'' = -0.876 \pm 0.067 \text{ km s}^{-1}\text{kpc}^{-3}.$$

The unit weight error is $\sigma_0 = 9$ km s^{-1}. Oort constants $A = 0.5R_0\Omega_0'$, $B = \Omega_0 + 0.5R_0\Omega_0'$ are: $A = 17.8 \pm 0.8$ km s^{-1}kpc^{-1} and $B = -13.2 \pm 1.5$ km s^{-1}kpc^{-1}. Using these values and taking into account the error $\sigma_{R_0} = 0.3$ kpc, we estimated the circular velocity of the Solar neighborhood $V_0 = |R_0\Omega_0| = 248 \pm 14$ km s^{-1} and its orbital period around the Galactic Centre $T = 2\pi/\Omega_0 = 198 \pm 11$ Myr.

Galactic rotational angular velocity $\Omega(R)$ and the corresponding linear circular velocity $V_\theta(R) = |R\Omega(R)|$ curves are shown in Figs. 3a and 3b, respectively.

As one can see from Fig. 3a, errors in parameters (16) lead to strongly increasing errors in the rotational angular velocity $\Omega(R)$ when $R > 10$ kpc. Due to this the confidence interval for the linear rotation curve $V_\theta(R)$ (Fig. 3b) starts to exceed the criterion adopted above, $dV_\theta = 20$ km s^{-1}, at $R > 10$ kpc. In general, we can conclude that the Galactic rotation curve found above approximates our initial data with fully adequate accuracy over the range of distances of $3 < R < 10$ kpc.

4.2 Periodic Perturbations

In Fig. 4, we present distribution of deviations from circular velocities ΔV_θ versus R obtained by subtraction of the rotation curve found above, with parameters (16), from the initial data. Fourier power spectra estimates (periodograms) of the sequence ΔV_θ ($|\overline{\Delta V_\theta}|^2$) and galactocentric radial velocities V_R ($|\overline{V_R}|^2$) versus wavelength λ are shown in Figs. 5a and 5b, respectively. In case of ΔV_θ, using two main low-frequency Fourier spectrum peaks extending up to $\lambda = 1.3$ kpc, we constructed an approximation curve of the residuals, as shown in Fig. 4. The amplitude of the approximation curve was fitted using a chi-square optimization technique. As it is seen from the picture, the approximation curve is not representative enough to make any conclusions.

But we have completely different situation in the case of radial velocities versus R shown in Fig. 6. In accordance
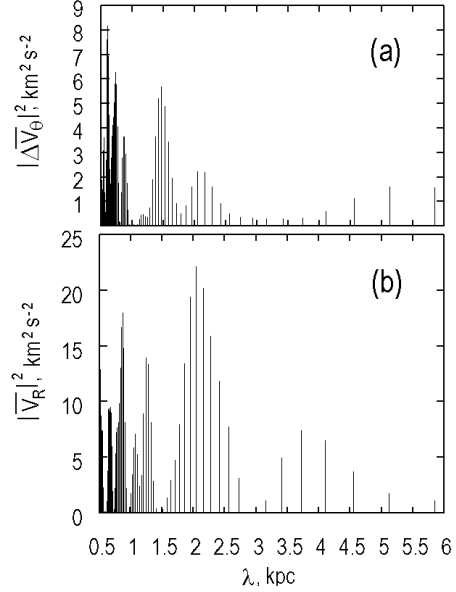
Figure 5. Periodograms of (a) deviations from circular velocities ΔV_θ and of (b) radial velocities V_R.

with the main periodogram peak shown in Fig. 5b, which is the largest one in the frequency region of interest, perturbations in radial velocities have an average wavelength of $\lambda = 2.0 \sim 0.25R_0$ kpc, which is in good agreement with results of other authors (see section 5.2). The approximation curve built using this main low-frequency Fourier spectrum peak extending from $\lambda = 3$ kpc to $\lambda = 1.5$ kpc and fitted using the chi-square optimization, is shown in bold in Fig. 6. One may clearly see that this curve gives the most exact description of radial velocities in the region of the Perseus arm ($R \approx 9$ kpc). In this region, extended as far as the location of the Sun, errors of amplitudes of radial velocities are less than ± 1 km s^{-1}. Peak value of the approximation curve reaches $f_R = 6.5$ km s^{-1} and at the area close to the Sun it is about 4.2 km s^{-1}. Confidence intervals for the approximation curve were determined using Monte-Carlo simulation for 1000 random samples. In agreement with the approximation curve, phase of the Sun lies in the interval $-140^o < \chi_\odot < -120^o$ with the mean value of $\chi_\odot \approx -130^o$. Radial perturbations in the Solar vicinity we estimate as periodic function with wavelength $\lambda = 2 \pm 0.2$ kpc and amplitude $f_R = 6.5 \pm 2$ km s^{-1}.

As it is seen from Fig. 5a and Fig. 5b both periodograms reveal peaks at wavelength $\lambda = 2$ kpc. We estimated probabilities p of belonging of these peaks to the periodic signal (not to noise) using simple formula derived by Vityazev (2001): $|\overline{V}(\lambda)|^2/\sigma_0^2/M \geqslant -\ln(1-p)$, where $|\overline{V}(\lambda)|^2$ is periodogram peak value at wavelength of interest, σ_0^2 is dispersion of input data sequence, M is number of data. In the first case we obtained $p = 0.6$ and in the second case $p = 0.992$ what justified more reliable estimation of spiral wave parameters from V_R rather than from ΔV_θ.
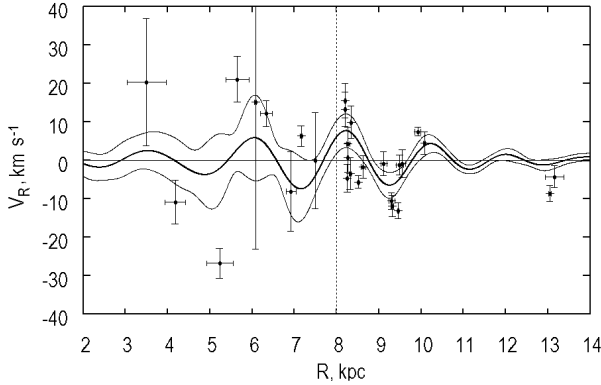
Figure 6. Radial velocities of masers V_R versus galactocentric distance R. Thin curves mark the confidence interval corresponding to 1σ level. Vertical line indicates the galactocentric distance of the Sun $R_0 = 8$ kpc.

4.3 Peculiar Solar Velocity with Respect to the LSR

In Fig. 7, spatial velocities U^1 and V^1 (see Table 1), free from Galactic rotation according to parameters (16), are given. Residual velocity components averaged over 28 masers are $\overline{U}^1, \overline{V}^1, \overline{W}^1 = (-8.6, -13.6, -7.5) \pm (2.1, 1.6, 1.3)$ km s^{-1}, with dispersion vector $(\sigma_{U^1}, \sigma_{V^1}, \sigma_{W^1}) = (10.8, 8.7, 6.8)$ km s^{-1}.

As one may see from this figure, residual velocities of most of masers form a sufficiently compact ellipse of smaller dispersion. Most of deviations from this compact distribution are due to the following three masers: G23.66−0.13, G23.43−0.18 and NGC 1333 (f2). The detail NGC 1333 (f2) reflects inner velocity dispersion within maser NGC 1333 which itself forms an expanding shell (Hirota et al., 2008a). Maser G23.66−0.13 has significantly negative radial velocity which reflects a certain peculiarity in its motion.

Excluding these three sources, for 25 masers forming a compact ellipse, we deduced the following mean velocity $\overline{U}^1, \overline{V}^1, \overline{W}^1 = (-9.1, -15.5, -8.5) \pm (1.9, 1.3, 1.2)$ km s^{-1}, with dispersion $(\sigma_{U^1}, \sigma_{V^1}, \sigma_{W^1}) = (9.3, 6.6, 6.1)$ km s^{-1}.

The question of great interest is how density wave perturbations affect the values of the LSR velocity components. Let us denote components of "non-perturbed" peculiar Solar velocity with respect to the LSR as $(U_\odot, V_\odot, W_\odot)_{\mathrm{LSR}}$. For the local case, i.e. for the immediate Solar neighborhood, under the condition $\chi \approx \chi_\odot$ we have

$$\overline{U}^1 = -(U_\odot)_{\mathrm{LSR}} - V_R \cos\theta + \Delta V_\theta \sin\theta, \qquad (17)$$

$$\overline{V}^1 = -(V_\odot)_{\mathrm{LSR}} + V_R \sin\theta + \Delta V_\theta \cos\theta. \qquad (18)$$

When $\theta \to 0$ ($R \approx R_0$), we have $\sin\theta \to 0$ and $\cos\theta \to 1$. Then

$$\overline{U}^1 = -(U_\odot)_{\mathrm{LSR}} + f_R \cos\chi_\odot, \qquad (19)$$

$$\overline{V}^1 = -(V_\odot)_{\mathrm{LSR}} + f_\theta \sin\chi_\odot, \qquad (20)$$

where $f_R, f_\theta > 0$. As one can see from (19)–(20), signs of corrections caused by spiral density waves are determined only by signs of $\cos\chi_\odot$ and $\sin\chi_\odot$. Adopting that: mean amplitudes of spiral density wave perturbations in both tangential and radial velocities are 6.5 ± 2 km s^{-1} and $\chi_\odot = -130^o \pm 10^o$, we obtain, according to (19)–(20), the

following "non-perturbed" velocity of $(U_\odot, V_\odot, W_\odot)_{\mathrm{LSR}} = (5.5, 11, 8.5) \pm (2.2, 1.7, 1.2)$ km s^{-1}. This result agrees with the estimate of Solar motion by Schönrich et al. (2010) and Francis & Anderson (2009).

We could not determine the value of $\chi_\odot$ using deviations from circular velocities of masers. But in order to confirm our results obtained above using Galactic radial velocities V_R of masers, we analyzed also a sample of Open Star Clusters (OSCs) from the compilation of Bobylev et al. (2007) which was based on the catalog of Piskunov et al. (2006), along with the line-of-sight velocities from the CRVOCA catalog (Kharchenko et al., 2007). We selected 117 young OSCs (age < 50 Myr) in radius $r < 2$ kpc using the following restriction for modulus of residual velocities: $\sqrt{\Delta U^2 + \Delta V^2 + \Delta W^2} < 50$ km s^{-1}.

Results of analysis of deviations from circular velocities ΔV_θ using Galactic rotation parameters (16) and galactocentric radial velocities V_R are shown in Figs. 8a and 8b, respectively. We can see a good agreement between the approximation curves shown in panels (a) and (b): wavelengths are almost similar, difference in phase is about $\pi/2$, peaks are also comparable (6-8 km s^{-1}). Periodograms of deviations from circular velocities and radial velocities are shown in Fig. 9. To obtain approximation curves in Fig. 8, we used low-frequency Fourier spectra up to wavelengths $\lambda = 1.3$ kpc and fitted the amplitude of perturbations using the chi-square optimization. Spectral analysis of V_R (Fig. 9b) reveals periodic motion with wavelength $\lambda = 1.9(0.23R_0)$ kpc. Spectral analysis of ΔV_θ (Fig. 9a) displays three dominant peaks at wavelengths $\lambda = 2.21(0.28R_0), 1.1(0.13R_0), 0.47(0.058R_0)$ kpc (compare with results by Clemens (1985):$\lambda = 0.22R_0, 0.12R_0, 0.05R_0$).

Now we can compare these results with those obtained using radial velocities V_R of masers. We can see a good agreement in the behavior of the approximation curves shown in Fig. 8b and Fig. 6 in the Solar area. Fourier spectrum of radial velocities of masers V_R reveals a dominant peak of amplitude 6.5 km s^{-1} at wavelength 2 kpc. In addition, there is a good agreement of phase $\chi_\odot \approx -120^o$ using data shown in Fig. 8b with the result obtained from masers $\chi_\odot \approx -130^o \pm 10^o$.

5 DISCUSSION

5.1 Galactic Rotation Curve

The shape of the Galactic rotation curve obtained above is in a good agreement with the one obtained by Zabolotskikh et al. (2002) for $R_0 = 7.5$ kpc as a result of thorough reconciliation of distance scales of different star groups. The value $\Omega_0 = -31.0 \pm 1.2$ km s^{-1}kpc^{-1} (see solution (16)) is in a good agreement with the following result obtained from 18 masers: -29.9 km s^{-1}kpc$^{-1} < \Omega_0 < -31.6$ km s^{-1}kpc^{-1} (McMillan & Binney, 2010) and with $\Omega_0 = -30.3 \pm 0.9$ km s^{-1}kpc^{-1} (Reid et al., 2009). Our value $V_0 = 248 \pm 14$ km s^{-1} ($R_0 = 8$ kpc) is in a good agreement with 254 ± 16 km s^{-1} ($R_0 = 8.4$ kpc) by Reid et al. (2009) and 244 ± 13 km s^{-1} ($R_0 = 8.2$ kpc) by Bovy et al. (2009).
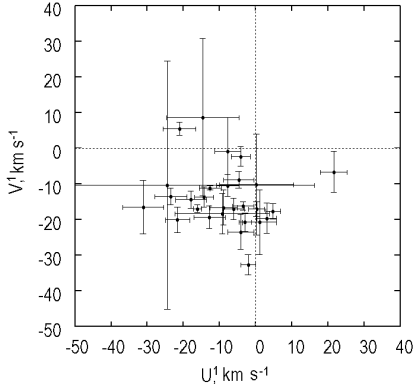
Figure 7. Heliocentric spatial velocities U^1 and V^1 free from Galactic rotation with parameters (16).

Figure 8. Deviations from (a) circular velocities ΔV_θ and (b) radial velocities V_R for 117 young OSCs versus galactocentric distance R. Approximation curves are shown with solid lines. Vertical line indicates galactocentric distance of the Sun $R_0 = 8$ kpc.

Figure 9. Periodograms of deviations from (a) circular velocities ΔV_θ and (b) radial velocities V_R for 117 young OSCs.

5.2 Spiral Structure Parameters

The estimate $\lambda = 0.22R_0$ of the distance between adjacent spiral arms was obtained by Clemens (1985). For $R_0 = 8.5$ kpc used here it gives $\lambda = 1.8$ kpc which is in a good agreement with the value $\lambda = 2.0$ kpc obtained in our study using 28 selected masers, as well as with $\lambda = 1.9$ obtained from 117 young OSCs. Mel'nik et al. (2001) obtained the estimate $\lambda = 2.0 \pm 0.2$ kpc by analyzing velocities of OB associations in the 3-kpc Solar neighborhood. An independent estimate $\lambda = 1.7 \pm 0.5$ kpc was obtained from the analysis of V_R velocities of young OSCs in the distance range of $6 < R < 9$ kpc (Bobylev et al., 2008).

From the analysis of OB stars and Cepheids, Byl & Ovenden (1978) found the following parameters of the Galactic spiral structure $f_R = 3.6 \pm 0.4$ km s^{-1} and $f_\theta = 4.7 \pm 0.6$ km s^{-1}, $\chi_\odot \approx 165 \pm 1°$, $i = -4.2 \pm 0.2°$. According to Clemens (1985), the value of perturbation amplitude is $|f_\theta| = 5$ km s^{-1} at **the** wavelength of $\lambda = 0.22R_0$.

Using Cepheids, Mishurov et al. (1997) found the following parameters: $f_R = 6.3 \pm 2.4$ km s^{-1} and $f_\theta = 4.4 \pm 2.4$ km s^{-1}, $\chi_\odot \approx 290 \pm 16°$, $i = -6.8 \pm 0.7°$. Using Hipparcos OB stars and Cepheids, Fernández et al. (2001) showed that amplitudes f_R and f_θ are about $6 - 4$ km s^{-1} and $20° < \chi_\odot < 284°$. Mean amplitude of radial perturbations $f_R = 6.5 \pm 2$ km s^{-1} found by us using masers is in a good agreement with the estimates listed above.

Location of the Sun in the external part of the Carina–Sagittarius arm is in agreement both with the distribution of stars and gas (Russeil, 2003) and with density wave theory.

5.3 Peculiar Velocity of the Sun

It is worth mentioning some results of determination of the non-perturbed LSR velocity parameters obtained simultaneously with parameters of the Galactic rotation, taking into account perturbations evoked by the spiral wave density. For example, these are: $(U_\odot, V_\odot)_{\rm LSR} = (2,5) \pm (2,2)$ km s^{-1} (Mishurov et al., 1997); $(U_\odot, V_\odot)_{\rm LSR} = (7.8, 13.6) \pm (1.3, 1.4)$ km s^{-1} (Mishurov & Zenina, 1999); $(U_\odot, V_\odot)_{\rm LSR} = (9, 12) \pm (1, 1)$ km s^{-1} (Lépine et al., 2001). Let us mention also the results of Fernándes et al. (2001), obtained using different samples of OB stars: $(U_\odot, V_\odot, W_\odot)_{\rm LSR} = (8.8, 12.4, 8.4) \pm (0.7, 1.0, 0.5)$ km s^{-1} and of Cepheids: $(U_\odot, V_\odot, W_\odot)_{\rm LSR} = (6.5, 10.4, 5.7) \pm (1.2, 1.9, 0.7)$ km s^{-1}.
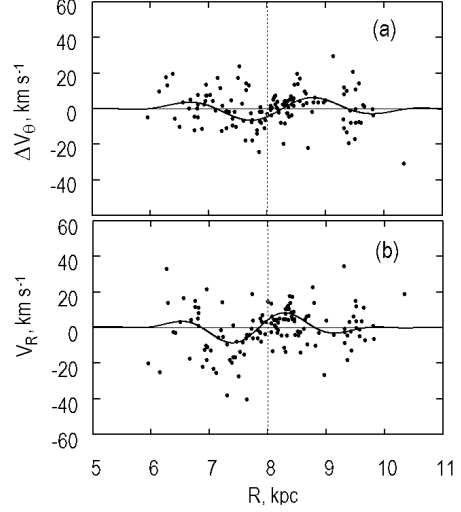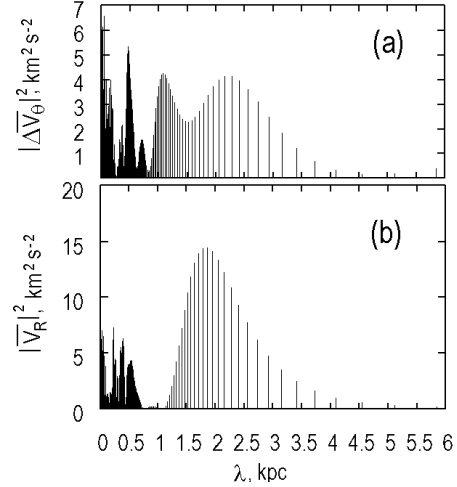
From the results listed here, we can see that values of (U, V) components of the LSR velocity are always smaller than the corresponding components of the standard Solar motion velocity $(U_\odot, V_\odot, W_\odot) = (10.3, 15.3, 7.7)$ km s^{-1}.

6 CONCLUSIONS

Spatial velocities of all currently known 28 masers having estimates of trigonometric parallaxes are reanalyzed. To determine the Galactic rotation curve, we used the first three terms of Taylor expansion of the Galactic angular rotational velocity at the galactocentric distance of the Sun $R_0 = 8.0$ kpc. Coefficients obtained from Bottlinger's equations are: $\Omega_0 = -31.0 \pm 1.2$ km s^{-1}kpc^{-1}, $\Omega_0' = 4.46 \pm 0.21$ km s^{-1}kpc^{-2}, $\Omega_0'' = -0.876 \pm 0.067$ km s^{-1}kpc^{-3}. Oort constants are $A = 17.8 \pm 0.8$ km s^{-1}kpc^{-1} and $B = $

-13.2 ± 1.5 km s^{-1}kpc^{-1}, which allowed us to estimate the circular velocity of the Solar neighborhood rotation $V_0 = 248 \pm 14$ km s^{-1} ($R_0 = 8$ kpc).

It was found that deviations from circular velocities ΔV_θ of masers are not representative enough for any reliable analysis, while the study of galactocentric radial velocities V_R of masers allowed us to estimate a number of useful parameters concerning spiral structure of the Galaxy. Based on Fourier analysis of velocities V_R, we obtained that: there are periodic perturbations evoked by the spiral density wave, with wavelength of $\lambda = 2.0 \pm 0.2$ kpc and peak velocity of $f_R = 6.5 \pm 2$ km s^{-1} and velocity of 4 ± 1 km s^{-1} near the location of the Sun; phase of the Sun in the density wave is $\chi_\odot = -130^o \pm 10^o$, which proves that the Sun is located in the inter-arm space.

Adopting the parameters of spiral density wave found we determined the following non-perturbed Solar peculiar velocity with respect to the LSR: $(U_\odot, V_\odot, W_\odot)_{\mathrm{LSR}} = (5.5, 11, 8.5) \pm (2.2, 1.7, 1.2)$ km s^{-1}. In this connection, in the regions near the Sun, velocity component $(V_\odot)_{\mathrm{LSR}}$ is influenced mostly by negative perturbation ΔV_θ and has smaller value than the corresponding velocity component $V_\odot = 15.3$ km s^{-1} of the Standard Solar motion.

REFERENCES

Asaki Y., Deguchi S., Imai H., Hachisuka K., Miyochi M, and Honma M., 2007, Proc IAU, 3, 378

Aumer M., and Binney J.J, 2009, MNRAS 397, 1286

Avedisova V.S., 2005, Astron. Rep. 49, 435 (2005).

Baba J, Asaki Y., Makino J., Miyoshi M., Saiton R., and Wada K., 2009, APJ, 706, 471

Bobylev V.V., Bajkova A.T., and Lebedeva S.V., 2007, Astron. Lett. 33, 720

Bobylev V.V., Bajkova A.T., and Stepanishchev A.S., 2008, Astron. Lett. 34, 515

Bovy J., Hogg D.W., and Rix H.-W., 2009, APJ, 704, 1704

Bower G.C., Plambeck R., Bolatto A., McCrady N., Graham J.R., de Pater I., Liu M.C., and Baganoff F.K., 2003, APJ, 598, 1140

Burton W.B., and Bania T.M., 1974, A&A, 33, 425

Byl J.B., and Ovenden M.W., 1978, APJ, 225, 496

Clemens D.P., 1985, APJ, 295, 422

Dehnen W., and Binney J.J., 1998, MNRAS 298, 387

Famaey B., Jorissen A., Luri X., Mayor M., Udry S., Dejonghe H., and Turon C., 2005, A&A, 430, 165

Fernández D., Figueras F., and Torra J., 2001, A&A, 372, 833

Francis C., and Anderson E., 2009, New Astronomy, 14, 615

Ghez A.M., Salim S., Weinberg N.N., Lu J.R., Do T., Dunn J.K., et al., 2008, APJ, 689, 1044

Gillessen S., Eisenhauer F., Trippe S., Alexander T., Genzel R., Martins F., and Ott T., 2009, APJ, 692, 1075

Hirota T., Bushimata T., Choi Y.K., Honma M., Imai H., Iwadate K., Jike T., Kameno S., et al., 2007, PASJ, 59, 897

Hirota T., Bushimata T., Choi Y.K., Honma M., Imai H., et al., 2008a, PASJ, 60, 37

Hirota T., Ando K., Bushimata T., Choi Y.K., Honma M., Imai H., et al., 2008b, PASJ, 60, 961

Kharchenko N.V., Scholz R.-D., Piskunov A.E., Röser S., and Schilbach E., 2007, Astron. Nachr. 328, 889

Lépine J.R.D., Mishurov Yu.N., and Dedikov S.Yu., 2001, APJ 546, 234

Lin C.C., and Shu F.H., 1964, APJ, 140, 646

McMillan P.J. and Binney J.J., 2010, MNRAS, 402, 934

Mel'nik A.M., Dambis A.K., and Rastorguev A.S., 2001, Astron. Lett. 27, 521

Mishurov Yu.N., and Zenina I.A., 1999, A&A, 341, 81

Mishurov Yu.N., Zenina I.A., Dambis A.K., Mel'nik A.M., and Rastorguev A.S., 1997, A&A, 323, 775

Ogorodnikov K.F., 1965, *Dinamics of Stellar Systems*. Pergamon, Oxford

Piskunov A.E., Kharchenko N.V., Röser S., Schilbach E., and Scholz R.-D., 2006, A&A 445, 545

Reid M.J., Menten K.M., Zheng X.W., Brunthaler L., Moscadelli L., Xu Y., et al., 2009, APJ, 700, 137

Rohlfs K., 1977, *Lectures in density waves*. Springer-Verlag, Berlin

Russeil D., 2003, A&A, 397, 133

Rygl K.L.J., Brunthaler A., Reid M.J., Menten K.M., van Langevelde H.J., and Xu Y., 2010, A&A, 511, A2

Sandstrom K.M., Peek J.E.G., Bower C., Bolatto A.D., and Plambeck R., 2007, APJ, 667, 1161

Sato M., Hirota T., Honma M., and 30 coauthors, 2008, PASJ, 60, 975

Sato M., Hirota T., Reid M.J., Honma M., Kobayashi H., Iwadate K., Miyahi T., end Shibata K.M., 2010, PASJ, 62, 287

Schönrich R., Binney J., and Dehnen W., 2010, MNRAS, 403, 1829

Van Leeuwen F., 2007, *Hipparcos, the New Reduction of the Raw Data*. Springer, Dordrecht

Vityazev V.V., 2001, *Analysis of non-uniformly distributed time series*. Saint-Petersburg University Press, Saint-Petersburg (in Russian)

Zabolotskikh M.V., Dambis A.K., and Rastorguev A.S., 2002, Astron. Lett. 28, 454